Assessment of Mechanical Recycling Potential of Plastic Waste from End-of-Life LFP Battery Cases

recycling

MDPI

Article

Assessment of Mechanical Recycling Potential of Plastic Waste from End-of-Life LFP Battery Cases

Chiara Gnoffo [1], Rossella Arrigo [1], Valentina Piergrossi [2], Letizia Tuccinardi [2], Riccardo Tuffi [2,*] and Alberto Frache [1]

[1] Department of Applied Science and Technology, Polytechnic of Turin, Viale Teresa Michel 5, 15121 Alessandria, Italy; chiara.gnoffo@polito.it (C.G.); rossella.arrigo@polito.it (R.A.); alberto.frache@polito.it (A.F.)

[2] Department for Sustainability, Italian National Agency for New Technologies, Energy and Sustainable Economic Development (ENEA), Casaccia Research Center, Via Anguillarese 301, S. Maria di Galeria, 00123 Rome, Italy; valentina.piergrossi@enea.it (V.P.); letizia.tuccinardi@enea.it (L.T.)

* Correspondence: riccardo.tuffi@enea.it

Abstract

This study evaluated the feasibility of mechanical recycling of plastic waste recovered from the disassembly of end-of-life lithium iron phosphate battery cases. In particular, the work focused on the case fraction, corresponding to the outer battery envelope, which represents the largest share of the plastic waste by weight. A preliminary characterization was carried out to determine the physico-chemical properties of the material and assess its suitability for mechanical recycling. The polymer matrix was found to consist of polypropylene, with glass fibers and calcium carbonate as inorganic fillers, each present at 18 wt%. X-ray fluorescence and elemental analysis confirmed the absence of elements of concern and subsequently, recycled material processability was investigated, with particular attention to injection molding, the same technology used to manufacture the original battery cases. Rheological analyses confirmed that the material exhibits Newtonian rheological behavior, suitable for injection molding, as also supported by a melt flow index value equal to 7.5 g/10 min (230 °C, 2.16 kg). The material was then reprocessed, and the resulting specimens were subjected to mechanical tests, with impact energy equal to 30.5 kJ/m^2 and flexural strength amounting to 36.8 MPa. Overall, the recycled material exhibited adequate processability and mechanical performance after one reprocessing step, suggesting its potential for high-value mechanical recycling.

Keywords: plastic waste; battery case; mechanical recycling; injection molding; reprocessing

Academic Editor: Denis Rodrigue

Received: 24 June 2026
Revised: 14 July 2026
Accepted: 15 July 2026
Published: 24 July 2026

1. Introduction

The significant growth of electric vehicles (EV), aerospace applications and renewable energy systems has led to an ever-increasing demand for efficient and relatable solutions for energy storage. The structures of battery cases play a crucial role in protecting and setting battery packs, and they ensure safe operation and long service life [1].

The selection of the right plastic is based on several fundamental properties, such as resistance to chemicals, high temperature, mechanical stresses and weathering phenomena, as well as low cost. Moreover, the use of lightweight materials as polymers ensures considerable weight savings, in addition to improving energy density and temperature control, simplifying assemblage and increasing impact resistance.

Among several polymers, polypropylene (PP) is the preferred option because of its excellent resistance to a wide range of chemicals including acid and alkaline ones. Furthermore, its ability to endure high and low temperatures and its low density make this polymer suitable for being used in battery cases [2]. These excellent properties are customized by the introduction of fillers with several shapes, as particulates or fibers. As widely known in literature [3,4], composites offer ideal advantages, particularly for battery-related applications, since they have a high strength-to-weight ratio that ensures excellent structural integrity and weight reduction. Glass fibers can be employed as a filler for the PP matrix with the aim to enhance mechanical properties and wear resistance [5,6]. In addition, polymeric material often contains flame-retardant additives, which are introduced during production so as to reduce flammability, especially for technologies concerning batteries [7,8].

The introduction of these fillers, very different from each other in terms of shape and composition, poses important safety problems, issues and concerns when it comes to end-of-life.

In general, lithium-ion batteries are governed from production to end-of-life by Regulation 2023/1542 of the European Parliament (EU) and of the Council on batteries and battery waste, as amended [9]. This regulation focuses primarily on the recovery of critical battery materials, such as lithium, cobalt and nickel, while referring to other legislations about restrictions on chemicals in plastics, such as flame retardants and/or hazardous substances in plastic waste.

When it comes to polymeric waste in general, Directive 2008/98/EC (Waste Framework Directive), as amended [10], regulates wastes in terms of classification and introduces the concept of End-of-Waste (EoW). On a technical level, Report 139303—End-of-waste plastic waste conducted by Joint Research Centre (JCR) [11] proposes common technical criteria at the European level to regulate and control plastic waste throughout the recycling chain, and it focuses also on the quality of the recyclates, setting a 2 wt% limit for the presence of other polymers as second phases.

A key aspect concerns the chemical safety of recycled materials. In this context, chlorinated (CFR) and brominated flame retardants (BFR) are regulated by Regulation 2019/1021 of the European Parliament (EU) and of the Council on persistent organic pollutants (POPs) [12], as amended, which restricts the use of these compounds to just a few hundred ppm since they are known to endanger human health and the environment. In addition, Directive 2011/65/EU on Restriction on the use of certain hazardous substances in electrical and electronic equipment (RoHS) [13], as amended, might become relevant when the recycled polymer is reused in such applications. Therefore, the recyclates must comply with the limits on such substances (brominated organic compounds and heavy metals). Regarding bromine, from a regulatory and technical perspective, the European Standard CEI EN 50625 for waste of electrical and electronical equipment (WEEE) collection, logistics, and treatment [14] establishes a 2000 ppm threshold for total bromine in WEEE plastic fractions as an operational criterion for the segregation of plastics containing brominated flame retardants. As reported by Sofies [15], this threshold was introduced because exceedance of the concentration limits for restricted BFRs is considered statistically unlikely below this value.

Previous studies on lithium-ion battery recycling have mainly focused on the optimization of mechanical pretreatments and on the recovery of valuable fractions. For example, Rademacher et al. [16] investigated how foam composite components in lithium-ion battery packs affect mechanical recycling efficiency and product quality, while Yun et al. [17] reviewed combined mechanical and metallurgical routes for recycling EV lithium-ion battery packs, mainly addressing dismantling, separation, and recovery of valuable metals and

active materials. Similarly, Kaas et al. [18] studied how shredder and mill settings influence black mass yield, Ni and Li recovery, separator foil recovery, casing recovery, and the separation behavior of anode and cathode fractions.

In parallel, other works have specifically addressed polypropylene recovered from lead-acid battery casings, in order to investigate the degradation behavior of virgin and recycled isotactic polypropylene used in lead-acid battery casings [19], or to study the presence and effect of Pb and other elements in recycled PP used for manufacturing new lead-acid battery cases [2]. More recently, Dong et al. [20] proposed a decontamination and modification strategy to recover, purify, and upgrade polypropylene from waste lead-acid batteries into higher-value recycled PP.

Overall, these studies show that the mechanical recycling of lithium-ion batteries has been mostly directed toward black mass, metals, electrodes, separator foils, and general casing recovery, while the recycling of PP battery casings has been mainly investigated for lead-acid batteries. However, to the best of the authors' knowledge, the mechanical recycling and injection molding reprocessing of the PP-based plastic case fraction recovered from end-of-life LFP battery cases remains scarcely investigated.

The aim of this work is to check the feasibility of recycling plastic waste coming from disassembly of end-of-life battery cases. In particular, the study addresses the research question of whether this plastic fraction can be mechanically recycled through the same processing technology used to produce the original battery case, namely injection molding. The working hypothesis is that, if the recovered plastic waste shows suitable physicochemical properties, absence of elements of concern, adequate processability, and acceptable mechanical performance after reprocessing, it can be considered suitable for high-value mechanical recycling. Firstly, several preliminary characterizations were carried out to assess the physico-chemical properties of the material and to evaluate its potential hazard and the characteristics that would make it suitable for mechanical recycling. After this general characterization, also based on the analysis of its processability, the possibility to recycle the material through the same processing technology used to produce the battery case, namely injection molding, was assessed. Finally, injection-molded specimens were produced and mechanically tested to evaluate the performance of the reprocessed material and its potential for high-value mechanical recycling.

2. Results and Discussion

2.1. Characterization of the Recovered Material

Figure 1 reports the FTIR spectrum of the battery case, while Table 1 lists the assignments of the majority of the peaks. From analysis of the spectrum, it can be noticed that most of the peaks are associated with the polymeric matrix [21–23], while three peaks can be associated with the presence of $CaCO_3$ [24]. Moreover, several peaks, albeit low, are detected in the 1000–1100 cm^{-1} region, related to Si-O-Si stretching, and in the 800–850 cm^{-1} area because of Si-O-Si bending [25].

Figure 2 shows two SEM micrographs at different magnifications. As clearly observable, the polymeric matrix contains at least two different fillers, with distinct shapes, dimensions, and structure. Specifically, an irregularly shaped granular filler and a fibrous reinforcement with an average diameter of approximately 20 µm are observed. The presence of several voids and cavities indicates poor interfacial adhesion between the fibers and the PP matrix, leading to fiber pull-out during sample fracture for SEM preparation.

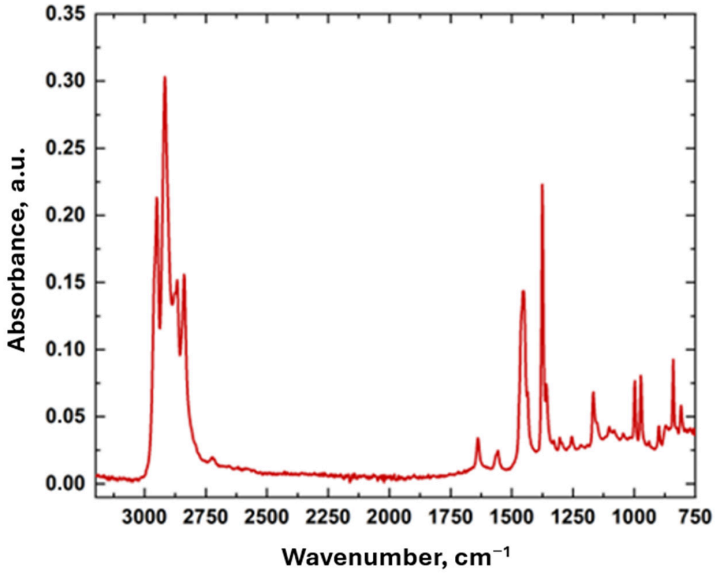

Figure 1. Fourier Transform Infrared Spectroscopy spectrum of battery case from 3200 cm^{-1} to 750 cm^{-1}.

Table 1. Analysis of peaks detected through spectroscopic analysis on battery case.

Peak/Band (cm^{-1})	Assignment	From
2949	CH_3 asymmetric stretching	PP
2919	CH_2 asymmetric stretching	PP
2864	CH_3 symmetric stretching	PP
2836	CH_2 symmetric stretching	PP
1448	CH_3 asymmetrical bending	PP
1375	CH_3 symmetrical bending	PP
1166	CH_2 twisting and CH wagging	PP
997	CH bending and wagging, CH_3 rocking	PP
972, 899	CH_3 rocking, CH bending and CH_2 wagging	PP
840, 808	CH_2 rocking and C-CH_3 stretching	PP
1430	Asymmetric CO_3^{2-} deformation	$CaCO_3$
875	Asymmetric CO_3^{2-} deformation	$CaCO_3$
713	Symmetric CO_3^{2-} deformation	$CaCO_3$
1000–1100	Si-O-Si stretching	Glass fibers
800–850	Si-O-Si bending	Glass fibers

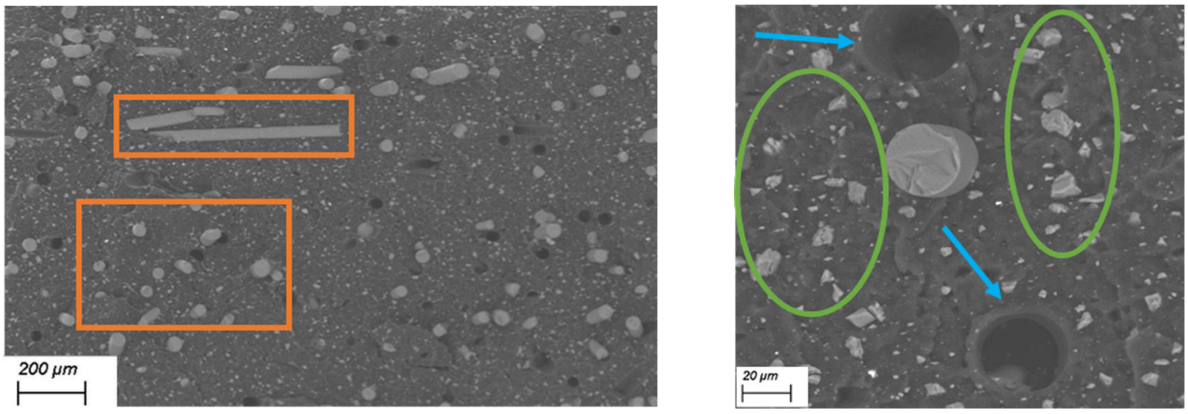

(**a**) (**b**)

Figure 2. Micrographs of battery case at 100× (**a**) and 1000× magnification (**b**). Orange rectangles highlight the presence of fibers, while blue arrows and green circles reveal voids and granular phase, respectively.

EDX analysis provided further insight into the chemical composition of the fillers, confirming the results of FTIR testing. The fibrous phase was found to consist mainly of silica and alkali and alkaline earth elements typically associated with glass, including Si, O, Na, Mg, and Ca, confirming the use of glass fibers in the battery case material. In addition, the granular phase was identified as calcium carbonate ($CaCO_3$), based on the detected presence of calcium, oxygen, and carbon. The combined use of glass fibers and $CaCO_3$ is common in battery cases, where glass fibers act as reinforcing agents, while $CaCO_3$ serves as a filler to enhance mechanical and thermal properties [26].

From proximate analysis, the plastic sample exhibited a moisture content of 0.6 wt% (Table 2). Although PP is generally considered a non-hygroscopic material, this moisture level is not sufficiently low to exclude potential issues such as porosity formation, thermal degradation, and melt instability during mechanical recycling processes, including extrusion and molding. Therefore, drying of the material prior to processing is recommended.

Table 2. Proximate and ultimate analysis of the battery case.

Moisture (wt%)	Ash I (wt%)	Ash II (wt%)	C (wt%)	H (wt%)	N (wt%)	S (wt%)	O * (wt%)	Cl (ppm)	Br (ppm)
0.6 ± 0.3	36 ± 1	28 ± 1	54.0 ± 0.3	9.2 ± 0.1	<0.02	<0.05	8.8	<20	<20

* Oxygen is calculated by difference, subtracting the sum of the other elements and the ash II content from 100.

Since FTIR and SEM EDX analyses highlighted the presence of both SiO_2 fibers and granular $CaCO_3$ within the polymeric matrix, ash quantification was performed in two steps. The residue after combustion at 550 °C (Ash I) was 36 wt%, corresponding to the total inorganic fraction, including $CaCO_3$. Upon further heating up to 900 °C, $CaCO_3$ decomposed into CaO and CO_2, leaving a residue (Ash II) of 28 wt%. The difference between Ash I and Ash II therefore represents the amount of CO_2 released from $CaCO_3$ decomposition. By balancing the chemical reaction of $CaCO_3$ decomposition, the $CaCO_3$ content in the polymeric matrix was calculated to be 18 wt%, while the corresponding CaO content accounted for 10 wt% within Ash II. The remaining 18 wt% of Ash II was attributed to other inorganic materials, most likely SiO_2 glass fibers. Table 3 reports the macroscopic material composition of the battery case on a dry basis, under the assumption that the combusted fraction consisted exclusively of polypropylene, as supported by both the H/C ratio and FTIR analysis.

Table 3. Molecular composition of battery case on dry basis.

PP (wt%)	$CaCO_3$ (wt%)	SiO_2 (wt%)
63.6	18.2	18.2

Table 2 also reports the results of elemental analysis. Nitrogen and sulfur were below the detection limit of the instrument, while carbon, hydrogen and oxygen were present at concentration of 54 wt%, 9 wt% and 8.8 wt% respectively. Considering only the organic fraction, the carbon and oxygen contents were estimated to be 51.8 wt% and 3.0 wt%, respectively, after correction for the $CaCO_3$ contribution. Oxygen may be attributed to the presence of organic additives or ageing/oxidative phenomena; however, its concentration was relatively low. The H/C atomic ratio, equal to 0.18 and close to the theoretical value of 0.17 for PP [27], indicates that the organic fraction is almost exclusively composed of PP. The lower organic carbon and hydrogen contents compared to those expected for neat polypropylene (i.e., C ≈ 85 wt% and H ≈ 15 wt% [28]) are attributable to the presence of inorganic fillers, as confirmed by the significant ash content.

Considering the potential issues associated with halide contamination in plastic recycling, the concentrations of chlorine and bromine were determined by ion chromatography. The measured concentrations of Cl and Br in the trapping solution were below the calibration range of the instrument (1 ppm). When referred to the sample mass, this value corresponds to a concentration in the plastic material of <20 ppm, well below the maximum limit of 2000 ppm established by European Standard CEI EN 50625 [14]. Furthermore, XRF analysis did not reveal the presence of heavy metals such as Pb, Hg, Cd, or Cr, in compliance with the RoHS Directive, with calcium being the only element showing significant peaks. According to the existing Regulations, these results indicate that the investigated polymeric waste is suitable for recycling.

Lastly, Figure 3 reports the thermograms recorded during the heating and the cooling scans, while Table 4 lists the main thermal characteristics. As expected for a PP-based material, the curves show a melting peak in the range between 160 and 170 °C and a crystallization peak in the range 100–125 °C. Besides, the sample shows a crystallinity content of approximately 42%.

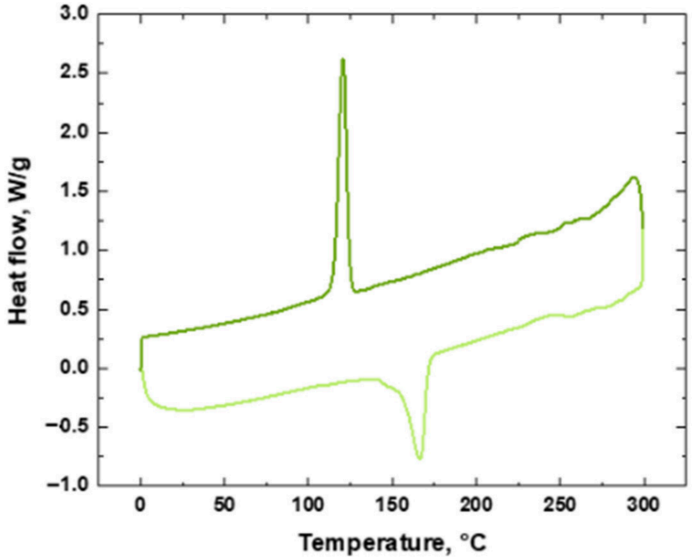

Figure 3. Heating and cooling curves (light and dark green, respectively) collected from differential scanning calorimetry analysis on battery case.

Table 4. Thermal properties of battery case.

T_C (°C)	ΔH_C (J/g)	T_M (°C)	χ (%)
120.7	61.5	166.5	42.3

2.2. Processability Assessment

To identify the most suitable processing technology for the material's mechanical recycling, its processability was evaluated through rheological analyses.

First, as assessed through MFI measurements, the material exhibited a melt flow index of 7.52 ± 0.18 g/10 min (230 °C, 2.16 kg), a value consistent with those typically reported in the literature for polymers suitable for injection molding [29].

The results of the frequency sweep test are shown in Figure 4. The material displays the characteristic shear-thinning behavior of pseudoplastic fluids, with a mild yield-like response at the lowest investigated frequencies attributable to the presence of the embedded fillers (particularly glass fibers) that hinder the relaxation of PP macromolecules [30]. The frequency dependence of the storage (G′) and loss (G″) moduli is also reported in Figure 4.

Overall, both moduli exhibit trends consistent with the presence of fibers. The deviations from Newtonian behavior observed at low frequencies can again be attributed to the influence of the fibers on polymer chain dynamics [31].

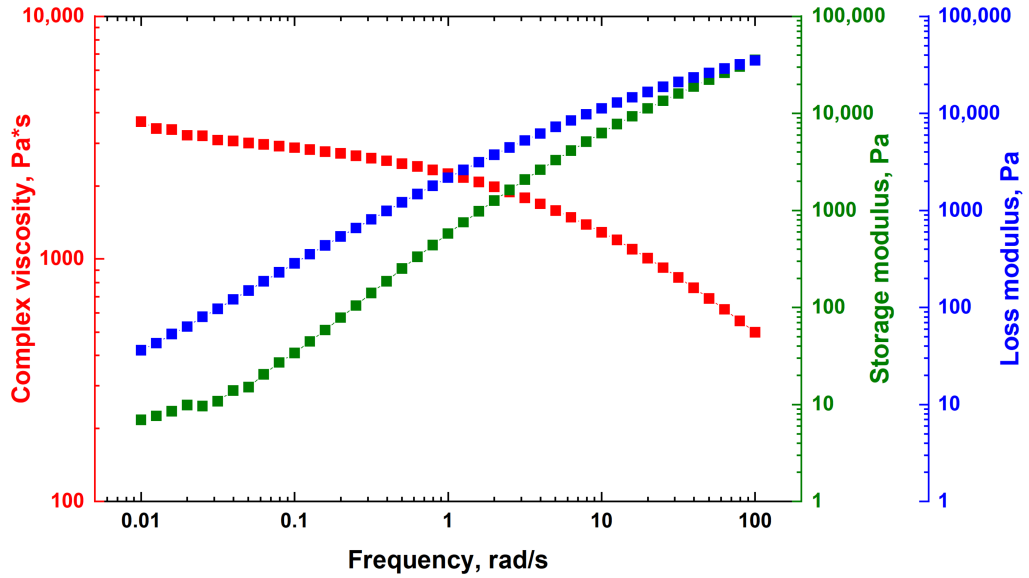

Figure 4. Rheological properties of battery case, in particular complex viscosity curve (red curve), storage modulus (green curve) and loss modulus (blue curve) as a function of frequency.

In principle, a polymer intended for injection molding should exhibit a well-developed Newtonian plateau, since a viscosity that remains relatively constant with changing shear conditions (and, indirectly, with pressure variations within the mold cavity) promotes stable flow and supports complete mold filling [32]. Accordingly, based on the behavior shown in Figure 4, the material can be considered suitable for injection molding: despite the presence of dispersed fillers, the melt retains the typical Newtonian response of PP, and the fillers do not markedly affect its flow characteristics.

2.3. Recycling of the Battery Case Through Injection Molding and Mechanical Characterization

Based on the preliminary characterization results and the processability assessment, the recovered material was reprocessed by injection molding to evaluate the feasibility of a recycling strategy capable of preserving its added value and avoiding downcycling.

To this aim, the injection molding conditions were set (see the processing parameters reported in Table 5), and specimens for different mechanical characterizations were produced (Figure 5).

Table 5. Processing parameters for injection molding of polypropylene battery case.

Parameter	Set Value
Injection pressure	650 bar
Injection time	0.23 s
Holding pressure	800 bar
Holding time	15 s
Barrel temperatures	210 °C–210 °C–210 °C–210 °C
Cooling time	20 s
Mold temperature	30 °C
Injection flow rate	60 cm^3/s

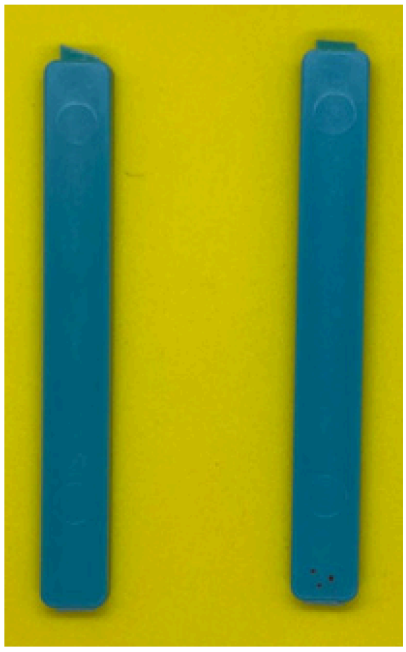

Figure 5. Specimens obtained through injection molding of battery case (10 mm × 4 mm × 80 mm).

Table 6 summarizes the results of the impact and flexural tests. Overall, the measured values are consistent with those commonly reported for injection-molded, glass-fiber-reinforced PP specimens [33,34] and with the typical increase in impact strength and storage modulus observed in polypropylene reinforced by glass fibers addition and/or filled with $CaCO_3$. For example, the flexural properties agree well with the data reported by Soudmand et al. [34] who found a flexural modulus of approximately 2000 MPa and a flexural strength of about 40 MPa, and with Peng et al. study [26] on PP filled with $CaCO_3$ particles at different loading levels, which demonstrated $CaCO_3$ as responsible for flexural modulus increase. These results indicate that, after one reprocessing step, the material exhibits mechanical performance consistent with that expected for filled/reinforced PP-based composites, supporting its potential for high-value mechanical recycling.

Table 6. Impact and flexural properties of injection-molded samples.

Impact Test	**Flexural Test**			
Impact energy (kJ/m^2)	Flexural modulus (MPa)	Flexural strength (MPa)	Maximum force (kN)	Strain at maximum force (%)
31 ± 1	2246 ± 10	36.8 ± 0.1	0.06 ± 0.01	5.5 ± 0.1

Figure 6 reports the main results of the DMTA analyses, namely the trend of storage and loss moduli, and tanδ as a function of the temperature. Additionally, the average values of loss and storage modulus evaluated at 30 °C are equal to 112 ± 17 MPa and 1792 ± 289 MPa, while HDT amounts to 80 °C. The moduli values are higher with respect to those usually reported for unfilled PP because of presence of fillers [33,35] and are consistent with the literature regarding PP-matrix composites with glass fibers [36]. Finally, the measured HDT is compatible with the reuse of the material in its original application, further supporting the feasibility of a high-value mechanical recycling strategy: in fact, it amounts to 80 °C, which is comparable with the values reported by Barczewski et al. [33] and Sadooghi et al. [37] for glass fibers and/or calcium carbonate reinforced PP composites, which report HDT always higher than 60 °C despite different percentages of filler.

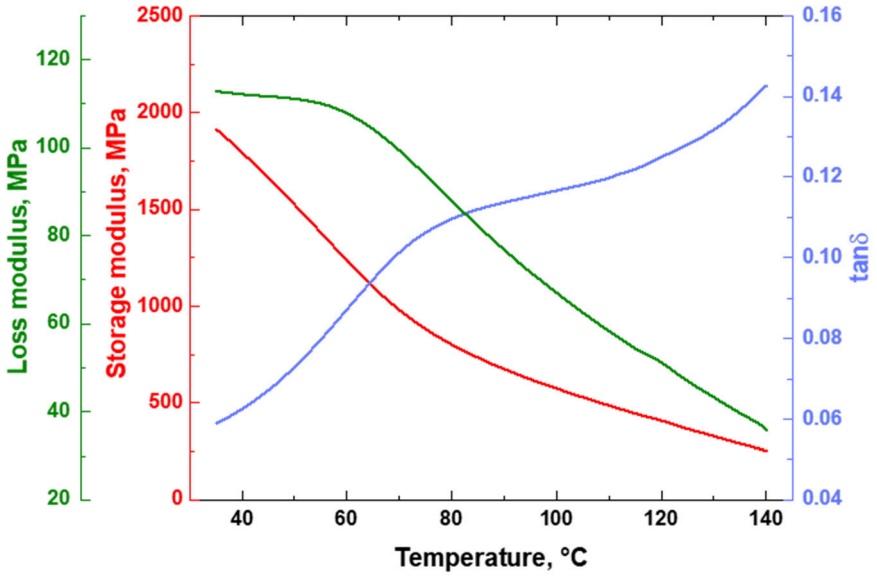

Figure 6. Dynamic mechanical thermal analysis curves of battery case, in particular loss modulus (green curve), storage modulus (red curve) and tanδ trend (blue curve) as a function of increasing temperature.

3. Materials and Methods

3.1. Materials

The lithium iron phosphate (LFP) end-of-life batteries (Figure 7), whose characteristics are reported in Table 7, were electrically discharged at a German recycling plant and subsequently shipped to the Casaccia Research Center of the Italian National Agency for New Technologies, Energy and Sustainable Economic Development (Rome, Italy). The batteries originated from automated forklifts and pallet trucks and belonged to the same production batch. A previous characterization carried out on individual batteries confirmed their consistency in terms of design, composition, and main characteristics. Six units were manually disassembled under a fume hood. Three main fractions were obtained: a plastic fraction consisting of case, tape, internal sachet and separator membrane; a metal fraction consisting of screws and bolts (ferrous metals), and portions of current collectors (copper and aluminum); and a cell fraction containing cathodes, anodes and electrolyte.

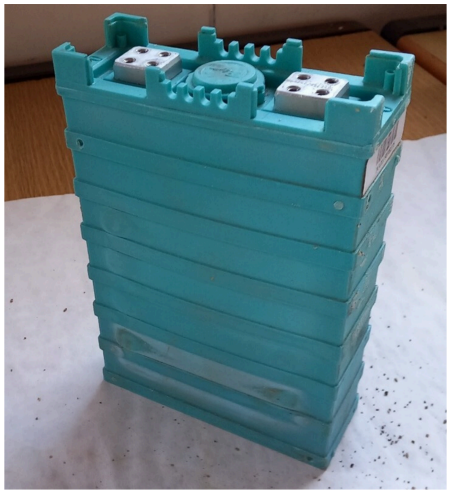

Figure 7. Lithium iron phosphate battery (125 mm × 45 mm × 175 mm).

Table 7. Characteristics of lithium iron phosphate batteries.

Cell Type	Voltage (V)	Dimension L × W × H (mm)	Weight (g)
Prismatic LFP cells	3.2	125 × 45 × 175	1395 ± 5

The different fractions were weighed to determine the percentage product composition, yielding the following results: plastics 29 wt%, metals 7 wt%, and cell 64 wt%. Among the plastic components, the case was proved to be the most relevant for recycling purposes accounting for 21 wt%.

The battery cases were roughly cut using a hand lever shear (Peddinghaus 3BR6, Paul Ferdinand Peddinghaus GmbH, Gevelsberg, Germany) to obtain pieces approximately 4–5 cm in size. The material was then processed with a cutting mill (Retsch SM 2000, Retsch GmbH, Haan, Germany) operated at 1500 rpm, in successive grinding stages using 10 mm and 4 mm sieves to create a single homogeneous plastic sample. A portion of the 4 mm fraction was further ground to 2 mm and finally sieved to obtain a powder with particle size < 0.5 mm for characterization analysis (Figure 8).

(**a**) (**b**) (**c**)

Figure 8. Batteries shredding: 40–50 mm fragments by hand lever shear (**a**); scraps < 4 mm by cutting mill (**b**); powder < 0.5 mm by cutting mill (**c**).

3.2. Processing

The material was processed through injection molding using a SmartPower 50 injection molding machine (WITTMANN BATTENFELD GmbH, Kottingbrunn, Austria). The processing conditions are resumed in Table 5, which are typical injection molding conditions reported in technical datasheets for filled PP. Prior to processing, the material was dried at 80 °C under vacuum overnight.

3.3. Characterization Techniques

The chemical composition of the plastic waste was evaluated using a combination of analytical techniques. Spectroscopic characterization was performed using a 4300 Handheld Fourier Transform Infrared Spectroscopy FTIR spectrometer (Agilent Technologies, Santa Clara, CA, USA) to investigate the polymeric nature of the plastic and the presence of organic and/or inorganic additives. Spectra were directly acquired on plastic fragments using 45 scans, a spectral resolution of 8 cm^{-1}, and a wavenumber range of 4000–650 cm^{-1}.

Morphological characterization was performed using a scanning electron microscope EVO 15 SEM (Carl Zeiss Microscopy GmbH, Oberkochen, Germany) with a lanthanum hexaboride (LaB6) filament. Prior to the SEM observations, the material was treated with liquid nitrogen to obtain brittle fracture surfaces, which were then gold sputtered.

Moreover, this instrument is equipped also with an Energy-dispersive X-ray (EDX) modulus to determine the chemical composition of the material.

A Vario MACRO Cube organic elemental analyzer (Elementar Analysensysteme GmbH, Langenselbold, Germany) was employed to determine the elemental composition of the samples in terms of carbon (C), hydrogen (H), nitrogen (N), and sulfur (S), while oxygen (O) was calculated by difference to 100 wt%. For this analysis, approximately 20 mg of powdered sample was weighed into tin boats together with an equal amount of oxidizing agent, namely tungsten trioxide (Elementar).

To assess the presence of brominated flame retardants (BFRs), the chlorine (Cl) and bromine (Br) contents were determined following EPA Method 5050. Specifically, 0.5 g compressed sample tablets were combusted in a C5000 Berthelot–Mahler calorimeter calorimetric bomb (IKA-Werke GmbH & Co. KG, Staufen, Germany) in the presence of a $NaHCO_3/Na_2CO_3$ buffer solution. After combustion, the resulting solution was analyzed by ion chromatography using an 883 Basic IC Plus ion chromatograph (Metrohm AG, Herisau, Switzerland).

Qualitative analysis of heavy metals was performed by X-ray fluorescence (XRF). An Olympus Delta system (Olympus Corporation, Tokyo, Japan), equipped with Innov X Delta Advanced software (version 2.5.20394), was used to detect inorganic elements with atomic number $Z \geq 15$.

Thermogravimetric analysis was carried out using a TGA/DSC 1 analyzer (Mettler Toledo, GmbH, Greifensee, Switzerland) to determine the moisture content, ash content at 550 °C, and ash content at 900 °C. This procedure enabled the discrimination of calcium carbonate ($CaCO_3$) from other inorganic constituents. Measurements were performed using 150 µL alumina crucibles containing approximately 50 mg of sample. Three replicates were analyzed for each sample. The experimental conditions adopted for the thermogravimetric tests are reported in Table 8.

Table 8. Thermogravimetric analysis thermal program for proximate analysis. Ash I and Ash II refer to the residue after combustion at 550 °C and after combustion at 900 °C, respectively.

Atmosphere	Temperature Program				Specific Content (wt%)
	T_i (°C)	T_f (°C)	$\beta = dT/dt$ (°C/min)	Δt Isotherm (min)	
N_2 at 60 mL/min	25		--	5	Moisture
	25	105	20	--	
	105		--	15	
Air at 90 mL/min	105	550	20	--	Ash I
	550		--	30	
	550	900	20	--	Ash II
	900		--	30	

Differential Scanning Calorimetry (DSC) tests were performed on approximately 8 mg of material incapsulated in sealed aluminum sample holder by using a DSC Q20 (TA Instruments, New Castle, DE, USA). The crystallinity content of the material was evaluated according to the following formula (Equation (1)):

$$\chi_C = 100 \frac{\Delta H_M}{\Delta H_{M100\%}(1 - x)} \quad (1)$$

where ΔH_M is the melting enthalpy, $\Delta H_{M100\%}$ is the melting enthalpy of the 100% crystalline PP (207 J/g [38]) and x is the second phase's content. A heating scan from 0 °C to 300 °C

with a temperature ramp equal to 10 °C/min was performed, followed by a cooling step at the same cooling rate.

The processability of the material was assessed by evaluating its Melt Flow Index (MFI) through a TWELVindex (ATR FAAR Industries S.r.l., Milan, Italy) instrument, working at 230 °C with a weight of 2.16 kg (in accordance with ISO 1131-1 [39]).

Rheological analysis was carried out by using an ARES parallel plate (diameter: 25 mm, gap: 1 mm) rotational rheometer (TA Instrument, New Castle, DE, USA). Frequency sweep tests were conducted at 210 °C in nitrogen atmosphere, with frequency ranging from 100 to 0.01 rad/s and with strain amplitude within the material linear viscoelastic range (preliminary assessed through strain sweep measurement carried out at 210 °C in nitrogen atmosphere and 1 rad/s).

Specimens obtained through injection molding were characterized from a mechanical point of view through the following measurements:

- impact test: this analysis was carried out by following ISO 180:2023 [40] with a Zwick-Roell HIT25P (Zwick Roell Group, Ulm, Baden-Württemberg, Germany) equipped with a 5.5 J pendulum on specimens with dimensions equal to 10 × 4 × 80 mm at room temperature. Three replicas were performed, and standard deviation was assessed.
- three-point bending test: it was performed according to ISO 178:2019 [41] by using an Instron 5966 machine (Instron, Norwood, MA, USA) equipped with a loading cell of 2 kN. Loading speed was set at 5 mm/min on 5 mm radius supports distanced 64 cm and, also in this case, three specimens were tested.
- Dynamic Mechanical Thermal Analysis (DMTA): DMA Q800 (TA Instruments, New Castle, DE, USA) was employed to perform frequency-strain DMTA analysis on injection-molded samples, in three replicates. The test was conducted at a constant frequency equal to 1 Hz, with a strain amplitude of 15 μm, temperature range from room temperature up to 140 °C and heating ramp of 2 °C/min. Storage modulus (E′), loss modulus (E″), mechanical damping factor tanδ and Heat Distortion Temperature (HDT) were evaluated; in particular, the HDT value was estimated as the temperature at which the storage modulus (E′) reaches 800 MPa, which corresponds to the approximation commonly adopted in the literature for this type of material [42].

4. Conclusions

This study provided a comprehensive preliminary characterization of the plastic battery case from end-of-life LFP batteries through chemical, physical, thermal, rheological, and mechanical analyses, with the aim of assessing its potential valorization through mechanical recycling and injection molding reprocessing. The results showed that halogen and heavy metal contents were below the detection limit and therefore within regulatory limits for recycling. The material was identified as a PP-based composite containing approximately 36 wt% fillers, mainly glass fibers and $CaCO_3$, and showed thermal stability up to about 400 °C. Melt flow index assessment showed a value equal to 7.5 g/10 min (230 °C, 2.16 kg) and demonstrated the suitability of the material for injection molding, enabling its reprocessing through the same technology used in the original manufacturing stage. After one injection molding reprocessing step, the material showed adequate mechanical performance for a recycled, highly filled PP-based composite, with a flexural modulus higher than 2240 MPa and an impact energy of about 30.5 kJ/m^2. DMTA analysis also indicated viscoelastic properties consistent with those expected for filled/reinforced PP-based materials. These results suggest that the recovered battery-case fraction retains promising processability and mechanical properties after reprocessing. Overall, the findings provide a first indication that the PP-based plastic fraction recovered from end-of-life

LFP battery cases may represent a promising candidate for high-value mechanical recycling and potential closed-loop applications.

The present study represents a preliminary technical validation based on a homogeneous and specific batch of LFP battery cases. Future investigations should include materials originating from different manufacturers and applications to assess the variability of recovered plastics and the broader applicability of the proposed recycling approach.

Author Contributions: Conceptualization, A.F. and R.T.; methodology, A.F., R.A. and R.T.; investigation, C.G., L.T. and V.P.; data curation, C.G.; writing—original draft preparation, C.G.; writing—review and editing, A.F., R.A., R.T., L.T. and V.P.; supervision, A.F. All authors have read and agreed to the published version of the manuscript.

Funding: This research was funded by Ministry of Enterprises and Made in Italy, within the Important Project of Common European Interest "European Battery Innovation" (EuBatIn), approved by the European Commission Decision C(2021) 494 final of 26 January 2021. Project No. IPCEI/006/00/B2, CUP B82C22000020001.

Data Availability Statement: The original contributions presented in this study are included in the article. Further inquiries can be directed to the corresponding author.

Conflicts of Interest: The authors declare no conflicts of interest.

References

1. Zhao, Y.; Shi, J.; Wang, K.; Wang, B.; He, C.; Deng, X. Mechanical Properties and Optimization Analysis on Battery Box with Honeycomb Sandwich Composite Structure. *Int. J. Automot. Technol.* **2023**, *24*, 1–14. [CrossRef]
2. Ferg, E.E.; Rust, N. The Effect of Pb and Other Elements Found in Recycled Polypropylene on the Manufacturing of Lead-Acid Battery Cases. *Polym. Test.* **2007**, *26*, 1001–1014. [CrossRef]
3. Azzopardi, B.; Hapid, A.; Kaleg, S.; Sudirja, S.; Onggo, D.; Budiman, A.C. Recent Advances in Battery Pack Polymer Composites. *Energies* **2023**, *16*, 6223. [CrossRef]
4. Alshammari, B.A.; Alsuhybani, M.S.; Almushaikeh, A.M.; Alotaibi, B.M.; Alenad, A.M.; Alqahtani, N.B.; Alharbi, A.G. Comprehensive Review of the Properties and Modifications of Carbon Fiber-Reinforced Thermoplastic Composites. *Polymers* **2021**, *13*, 2474. [CrossRef] [PubMed]
5. Siraj, S.; Al-Marzouqi, A.H.; Iqbal, M.Z.; Ahmed, W. Impact of Micro Silica Filler Particle Size on Mechanical Properties of Polymeric Based Composite Material. *Polymers* **2022**, *14*, 4830. [CrossRef] [PubMed]
6. Yadav, R.; Singh, M.; Shekhawat, D.; Lee, S.-Y.; Park, S.-J. The Role of Fillers to Enhance the Mechanical, Thermal, and Wear Characteristics of Polymer Composite Materials: A Review. *Compos. Part Appl. Sci. Manuf.* **2023**, *175*, 107775. [CrossRef]
7. Liu, W.; Jiang, Y.; Wang, N.; Fu, W. Recent Progress in Flame Retardant Technology of Battery: A Review. *Resour. Chem. Mater.* **2023**, *2*, 80–99. [CrossRef]
8. Kim, J.; Hyun, J.; Kim, S.; Park, W.H.; Yu, S. Phosphorus-Based Flame-Retardant Electrolytes for Lithium Batteries. *Adv. Energy Mater.* **2025**, *15*, 2500587. [CrossRef]
9. European Union. *Regulation (EU) 2023/1542 of the European Parliament and of the Council of 12 July 2023 Concerning Batteries and Waste Batteries, Amending Directive 2008/98/EC and Regulation (EU) 2019/1020 and Repealing Directive 2006/66/EC*; European Union: Brussels, Belgium, 2023.
10. European Union. *Directive 2008/98/EC of the European Parliament and of the Council of 19 November 2008 on Waste and Repealing Certain Directives*; European Union: Brussels, Belgium, 2008.
11. Pierri, E.; Egle, L.; Milios, L.; Saveyn, H. EU-Wide End-of-Waste Criteria for Plastic Waste. Available online: https://publications.jrc.ec.europa.eu/repository/handle/JRC139303 (accessed on 8 July 2026).
12. European Union. *Regulation (EU) 2019/1021 of the European Parliament and of the Council of 20 June 2019 on Persistent Organic Pollutants*; European Union: Brussels, Belgium, 2019.
13. European Union. *Directive 2011/65/EU on Restriction on the Use of Certain Hazardous Substances in Electrical and Electronic Equipment (RoHS II)*; European Union: Brussels, Belgium, 2011.
14. *EN 50625-1:2014*; Collection, Logistics & Treatment Requirements for WEEE—Part 1: General Treatment Requirements. CEI—Comitato Elettrotecnico Italiano: Milan, Italy, 2014.
15. Sofies. *Study on the Impacts of Brominated Flame Retardants (BFRs) on the Recycling of WEEE Plastics in Europe*; Sofies (Recently Acquired by DSS+ DuPont Sustainable Solutions+): Geneva, Switzerland, 2020.

16. Rademacher, P.; Kaas, A.; Wilke, C.; Peuker, U.A. Influence of Foam Composite in Lithium-Ion Battery Packs on Their Mechanical Recycling. *Next Sustain.* **2025**, *6*, 100208. [CrossRef]
17. Yun, L.; Linh, D.; Shui, L.; Peng, X.; Garg, A.; Le, M.L.P.; Asghari, S.; Sandoval, J. Metallurgical and Mechanical Methods for Recycling of Lithium-Ion Battery Pack for Electric Vehicles. *Resour. Conserv. Recycl.* **2018**, *136*, 198–208. [CrossRef]
18. Kaas, A.; Wilke, C.; Peuker, U.A. Influence of Shredder and Mill Settings on the Material Recoveries and Product Qualities of a Two-Stage Mechanical Recycling Process of Automotive Lithium-Ion Batteries. *Waste Manag.* **2025**, *204*, 114912. [CrossRef] [PubMed]
19. Rust, N.; Ferg, E.E.; Masalova, I. A Degradation Study of Isotactic Virgin and Recycled Polypropylene Used in Lead Acid Battery Casings. *Polym. Test.* **2006**, *25*, 130–139. [CrossRef]
20. Dong, L.; Zhi, W.; Dong, J.; Xie, H.; Li, F. From Waste Lead-Acid Batteries to High-Value Polypropylene: Sustainable Recovery and Enhancement via Decontamination and Modification Strategy. *J. Environ. Manag.* **2026**, *397*, 128280. [CrossRef] [PubMed]
21. Fang, J.; Zhang, L.; Sutton, D.; Wang, X.; Lin, T. Needleless Melt-Electrospinning of Polypropylene Nanofibres. *J. Nanomater.* **2012**, *2012*, 382639. [CrossRef]
22. Kamalanathan, P.; Ramesh, S.; Bang, L.T.; Niakan, A.; Tan, C.Y.; Purbolaksono, J.; Chandran, H.; Teng, W.D. Synthesis and Sintering of Hydroxyapatite Derived from Eggshells as a Calcium Precursor. *Ceram. Int.* **2014**, *40*, 16349–16359. [CrossRef]
23. Chibani, N.; Djidjelli, H.; Dufresne, A.; Boukerrou, A.; Nedjma, S. Study of Effect of Old Corrugated Cardboard in Properties of Polypropylene Composites: Study of Mechanical Properties, Thermal Behavior, and Morphological Properties. *J. Vinyl Addit. Technol.* **2016**, *22*, 231–238. [CrossRef]
24. Fathy, A.T.; Moneim, M.A.; Ahmed, E.A.; El-Ayaat, A.M.; Dardir, F.M. Effective Removal of Heavy Metal Ions (Pb, Cu, and Cd) from Contaminated Water by Limestone Mine Wastes. *Sci. Rep.* **2025**, *15*, 1680. [CrossRef] [PubMed]
25. Mawhinney, D.B.; Glass, J.A.; Yates, J.T. FTIR Study of the Oxidation of Porous Silicon. *J. Phys. Chem. B* **1997**, *101*, 1202–1206. [CrossRef]
26. Peng, Y.; Musah, M.; Via, B.; Wang, X. Calcium Carbonate Particles Filled Homopolymer Polypropylene at Different Loading Levels: Mechanical Properties Characterization and Materials Failure Analysis. *J. Compos. Sci.* **2021**, *5*, 302. [CrossRef]
27. Cuthbertson, A.A.; Lincoln, C.; Miscall, J.; Stanley, L.M.; Maurya, A.K.; Asundi, A.S.; Tassone, C.J.; Rorrer, N.A.; Beckham, G.T. Characterization of Polymer Properties and Identification of Additives in Commercially Available Research Plastics. *Green Chem.* **2024**, *26*, 7067–7090. [CrossRef]
28. Emifoniye, E.U.; Erameh, A.A.; Orhorhoro, E.K. Investigation of Proximate and Ultimate Analysis of Household Generated Plastic Waste for Feasible Design of a Pyrolysis Pilot Plant. *World J. Adv. Eng. Technol. Sci.* **2025**, *15*, 2107–2118. [CrossRef]
29. Shenoy, A.V.; Saini, D.R. Melt Flow Index: More than Just a Quality Control Rheological Parameter. Part I. *Adv. Polym. Technol.* **1986**, *6*, 1–58. [CrossRef]
30. Thomasset, J.; Carreau, P.J.; Sanschagrin, B.; Ausias, G. Rheological Properties of Long Glass Fiber Filled Polypropylene. *J. Non-Newton. Fluid Mech.* **2005**, *125*, 25–34. [CrossRef]
31. Nayak, S.K.; Mohanty, S.; Samal, S.K. Influence of Short Bamboo/Glass Fiber on the Thermal, Dynamic Mechanical and Rheological Properties of Polypropylene Hybrid Composites. *Mater. Sci. Eng. A* **2009**, *523*, 32–38. [CrossRef]
32. Wang, M.-L.; Chang, R.-Y.; Hsu, C.-H. *Molding Simulation: Theory and Practice*; Carl Hanser Verlag GmbH & Co. KG: Munich, Germany, 2018; ISBN 978-1-56990-620-0.
33. Barczewski, M.; Mysiukiewicz, O.; Andrzejewski, J.; Matykiewicz, D.; Medycki, D.; Kloziński, A.; Skórczewska, K.; Szostak, M. Thermo-mechanical and Mechanical Behavior of Hybrid Isotactic Polypropylene Glass Fiber Reinforced Composites (GFRC) Modified with Calcium Carbonate (CaCO3). *Polym. Eng. Sci.* **2020**, *60*, 1588–1603. [CrossRef]
34. Soudmand, B.H.; Shelesh-Nezhad, K. Experimental Investigation on the Mechanical Properties of Co-Polypropylene/GF/CaCO3 Hybrid Nanocomposites. *Polym. Sci. Ser. A* **2016**, *58*, 454–463. [CrossRef]
35. Carvalho, G.B.; Canevarolo, S.; De Sousa, J.A. Correlation of Fatigue Behavior and Dynamic Mechanical Properties of Hybrid Composites of Polypropylene/Short Glass Fibers/Hollow Glass Beads. *J. Thermoplast. Compos. Mater.* **2023**, *36*, 2233–2259. [CrossRef]
36. Amash, A.; Zugenmaier, P. Thermal and Dynamic Mechanical Investigations on Fiber-Reinforced Polypropylene Composites. *J. Appl. Polym. Sci.* **1997**, *63*, 1143–1154. [CrossRef]
37. Sadooghi, A.; Hashemi, S.J.; Zal, V.; Rahmani, F.; Rahmani, K.; Bodaghi, M. Advancing Mechanical Properties of Polypropylene Matrix Composites: Analysis of Diverse Reinforcing Fillers. *Polym. Adv. Technol.* **2025**, *36*, e70060. [CrossRef]
38. Gnoffo, C.; Arrigo, R.; Sisani, M.; Frache, A. Elongational Flow-induced Microstructure Evolutions in Polypropylene/Layered Double Hydroxides Nanocomposites. *Polym. Compos.* **2024**, *45*, 6606–6617. [CrossRef]
39. *ISO 1133-1:2022*; Plastics—Determination of the Melt Mass-Flow Rate (MFR) and Melt Volume-Flow Rate (MVR) of Thermoplastics—Part 1: Standard Method. International Organization for Standardization: Geneva, Switzerland, 2022.
40. *ISO 180:2023*; Plastics—Determination of Izod Impact Strength. International Organization for Standardization: Geneva, Switzerland, 2023.

41. *ISO 178:2019*; Plastics—Determination of Flexural Properties. International Organization for Standardization: Geneva, Switzerland, 2019.
42. D'Anna, A.; Arrigo, R.; Frache, A. PLA/PHB Blends: Biocompatibilizer Effects. *Polymers* **2019**, *11*, 1416. [CrossRef] [PubMed]